

Boiling Instabilities in Microtubes

Alihan KAYA¹, Mehmed Rafet ÖZDEMİR¹, Ali KOŞAR^{1,*}

* Corresponding author: Tel.: ++90 (216) 4839621; Fax: ++90 (216) 4839550; Email:
kosara@sabanciuniv.edu

1: Faculty of Engineering and Natural Sciences, Sabancı University, Istanbul, TURKEY

Abstract: Microprocessor and microchip speeds are continuously increasing with their shrinking sizes. For this reason, the size of subject related heat sinks are continuously decreasing from mini size to micro size. Among many microscale heat transfer cooling applications, the most practical and extensively used micro heat sinks are plain microchannels. This study addresses the lack of information about microchannel boiling instability phenomena and includes a parametric investigation in microtubes. Experimental data were obtained from a microtube having a 250- μm inner diameter, which was tested at low mass fluxes (78.9-276.3 $\text{kg/m}^2\text{s}$) to reveal potential boiling instabilities. De-ionized water was used as a coolant, while the microtube was heated by Joule heating. Configurations prone to boiling instabilities (low system pressures, low mass velocities) were imposed to observe boiling instabilities in microtubes. After the experiments without any inlet restriction, experiments were conducted with the configuration with inlet restriction where pressure drop over inlet restriction element was 4 times as much as pressure drop over the microtube. Temperature and pressure drop fluctuation signals were recorded and processed once boiling instabilities were observed.

Keywords: Micro Flow, Boiling Instabilities, Microtubes, Critical Heat Flux

1. Introduction

Over the last decade an astonishing progress in MEMS technology has been witnessed. From the aspect of microchannel exchangers, there are an increasing number of studies in the literature about flow boiling in small channels. As a result of this progress the demand for micro scale cooling devices has been proportionally increased. In this manner, two-phase flow boiling systems are becoming more important because of their highly efficient heat transfer capabilities, less pumping power requirement than single-phase liquid flow [1] and better controllability and reproducibility [2]. They are also handy in numerous microscale applications in addition to electronics cooling such as microchips in laptop computers [3], microreactors [4], fuel cells [5], drug delivery [6], micropropulsion [7], and automotive industry [6]. Such a large palette of applications is increasingly motivating the researchers towards understanding physics of microchannel flow boiling by employing plain microchannels as a

microscale cooling solution. However, working on such small scales comes with flow boiling instability problems particularly observed at low flow rates and pressures [8]. Flow boiling instabilities significantly affect the performance of micro fluidic systems and might lead to premature critical heat flux (CHF) [9, 10]. Two-phase flow heat transfer, flow pattern and pressure drop have been extensively investigated in the last decade [11-14]. In the studies reporting two-phase flow instabilities in single channels [15-17], wall temperature and pressure fluctuations were carefully received. Kennedy et al. [18] determined the onset of the instability by using pressure drop signals. Several authors also evidenced instabilities in single and parallel micro-channels [18-22]. Kandlikar [20] noted large amplitude fluctuations in multi-channel evaporators. Flow pattern observations revealed a flow reversal in some channels with expanding bubbles pushing the liquid-vapor interface in both upstream and downstream directions [19]. Qu and Mudawar [22] found two behaviors of fluctuations in a

set of parallel channels: The first, where the oscillations in the channels are in phase and the second, where the oscillations behave in a chaotic way. Consolini and Thome [23] explained such cyclical boiling behavior as liquid filling, bubble nucleation, growth and coalescence of bubbles, vapor expansion of vapor and evaporation of liquid film on walls.

For having an idea about how to manipulate bubble nucleation, Koşar et al. [24] performed a study about microchannels with artificial flow restrictions, which notes that heat fluxes corresponding to the onset of unstable boiling q_{oub} increases asymptotically. In the initial stage of the bubble nucleation cycle, i.e., during the rapid bubble growth, a spherical bubble grows until it attains a size comparable to the channel hydraulic diameter [25]. Kuo et al. mentioned that although the bubbly slug and annular flow patterns are similar as in macrochannels, the activation mechanism of bubble nucleation sites in microchannels is considerably different than in macroscale channels, which is possibly due to increasing bubble-departure-diameter to channel-hydraulic-diameter ratio in microchannels [2].

Another important fact that negatively affects the efficiency of a microtube heat exchanging system is the high pressure drop per unit length [26]. According to the study of Bergles and Kandlikar [27], the pressure drop profile from channel inlet to outlet demonstrates a low-high-low behavior, because of the changing L/D ratio and vaporization.

This study aims at extending current studies on the microchannel instability problems in single channel. To do this, experimental data were obtained from single microtube configurations. Experiments were conducted at relatively low mass fluxes (78,9-276,3 kg/m²s). De-ionized water was used as a working fluid, while the microtube was heated by Joule heating. After the experiments without any inlet restriction, experiments were conducted the same configuration with inlet restriction. Temperature and pressure drop fluctuation

signals were recorded and processed by using Data Acquisition System.

Nomenclature

A_c	Cross sectional area m ² .
G	Mass velocity kg m ⁻² s ⁻¹ .
\dot{m}	Mass flow rate kg s ⁻¹ .

2. Experimental Test Setup and Procedure

2.1 Experimental Test Setup

The experimental setup consists of the test section, a Nitrogen tank, a storage cylinder, a flow filter, Cole Palmer® flow meters, pressure sensors, proper tubing, fittings and a data acquisition system (DAQ). Two alligator clips, each 3 mm wide, were attached to the heated length on the microtube surface. They were installed with a prescribed distance (heated length) from each other and were connected to a high current power supply with an adjustable DC current and high power output to provide Joule heating to the 14.88 cm long micro tube of $\sim 254\mu\text{m}$ inner diameter. The heated length was adjusted to 5.65cm. The sealing between the microtube and the experimental loop was accomplished by Conax® packing glands consisting of a gland body and a sealant. The microtube was connected to the experimental loop from one side, whereas the other end was exposed to the atmosphere to ensure atmospheric conditions at the exit. At that point, the pressure for flow was provided with Nitrogen tube, rather than a pump or motor. To measure local temperatures, three thin Omega® thermocouple wires ($\sim 76\mu\text{m}$ thick) were carefully installed to the microtube surface at desired locations using Omega® Bond. Thermocouples were located at $x_{\text{th1}} = 1.82$ cm, $x_{\text{th2}} = 3.32$ cm and $x_{\text{th3}} = 4.82$ cm over the heated length of 5.65cm. Inlet pressures were measured manually via two Omega® pressure transducers with a 0 to 100 psi gauge pressure range. In the second step of the experiment, a restriction valve just before the microtube was inserted. A digital pressure

sensor was installed before the test section, which provides the measure pressure and is connected to DAQ (Data Acquisition System). Furthermore, flow rate data was obtained together with the voltage, current, and wall/fluid temperatures, pressures, which were acquired through a LabView® interface with time and were transferred to a spreadsheet file for data reduction.

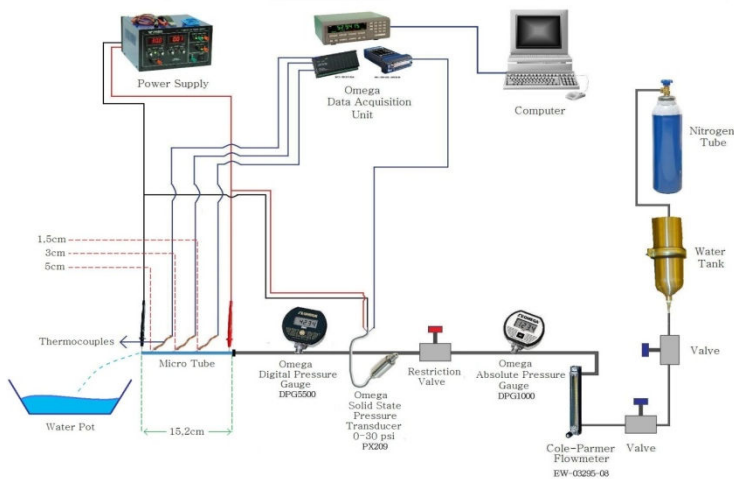


Figure 1: Schematic illustration of the whole experiment setup.

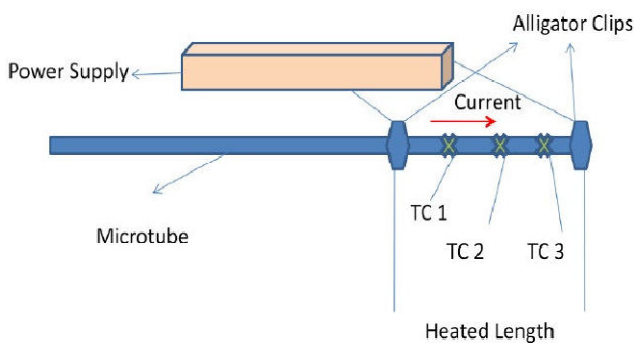


Figure 2: Schematic illustration of the heated length and the places of thermocouples

2.2 Experimental Procedure

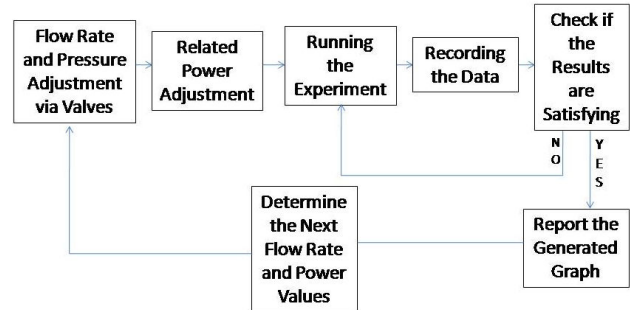


Figure 3: Flow chart schematic of the procedure

The experiment procedure necessitates working with a variety of fixed relatively low flow rates. Those flow rates were maintained by sensitive Nitrogen tank pressure and fine flow valve. After the fixed flow rates are maintained, the desired power is supplied from the power supply. The current was increased in ~ 0.5 A increments. Then the data were acquired via DAQ module with the rate of 100 data/s. Those gathered data were instantaneously transferred to the LabView® spreadsheet. The results were received, and used as input in the data reduction phase.

In the second stage of the experiments, a fine restriction valve was inserted before the microtube configuration. This addition is expected to reduce the instabilities by extending the boiling curve. After a sensitive adjustment of the restriction valve, the expected pressure restriction was adjusted (4:1) to produce significant pressure drop upstream the microtube. The rest of the procedure is the same as before.

To estimate small heat losses, electrical power was applied to the test section before any fluid flow and experiment. The temperature difference between the ambient and the test section was recorded along with the corresponding power at steady state so that the power could be found as a function of surface temperature to calculate the heat loss associated with each experimental data point.

3. Data Reduction

The data obtained from the voltage, current, flow rate, temperature and pressure measurements were used to analyze and interpret results.

G is the mass velocity and defined as:

$$G = \dot{m} / A_c \quad (1)$$

A_c is cross-sectional of the tube. The uncertainties of the measured value are given in Table 1. They were provided by the manufacturer's specification sheet.

Uncertainty	Error
Flow Rate, Q (for each reading)	$\pm 1.0 \%$
Voltage supplied by power source, V	$\pm 0.1 \%$
Current supplied by power source, I	$\pm 0.1 \%$
Temperature, T	$\pm 0.1^\circ\text{C}$
Electrical power, P	$\pm 0.15 \%$
Pressure drop, ΔP	$\pm 0.25 \%$
Mass flux, G	$\pm 2.7 \%$

Table 1 Uncertainties in experimental parameters

4. Results and Discussion

In Figs. 4-19 pressure and temperature fluctuations at different mass and heat fluxes are given just before the microtube was burned when the power was further increased. As can be seen from the figures, the difference between peak points of fluctuations shows a decreasing tendency as the flow rate increases. From the aspect of fluctuation periods, the fluctuation periods tend to increase by the increasing mass and heat flux, and the periods are longer in the setup without inlet restriction. Overall, the magnitude of the fluctuations is

lower than those reported in the literature [25]. However, it should be noted that the microtubes failed after a slight increase in the heat flux so that no further temperature and pressure signals could be attained beyond these points. Even though the CHF values of boiling curve was predicted to be extended when the inlet restrictions are introduced to system, the heat flux value rise was observed to be minor. Thus as a future research effort, more restriction ratio is to be introduced.

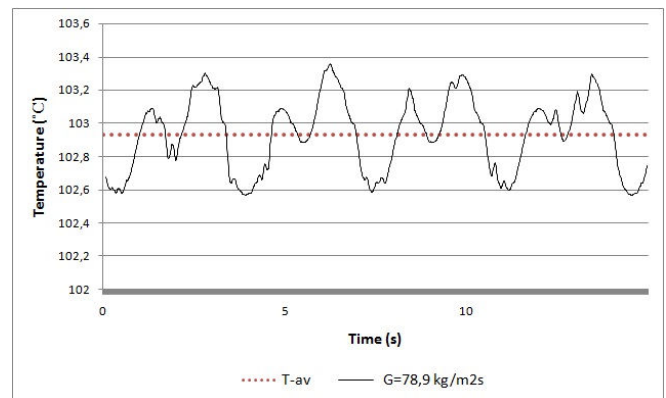


Figure 4: Temperature fluctuations in 0,254mm inner diameter microtube at $G=78,9 \text{ kg/m}^2\text{s}$ mass flux, $q''= 24,93 \text{ W/cm}^2$ heat flux, at Thermocouple 3. (Fluctuation period is approx. 4s)

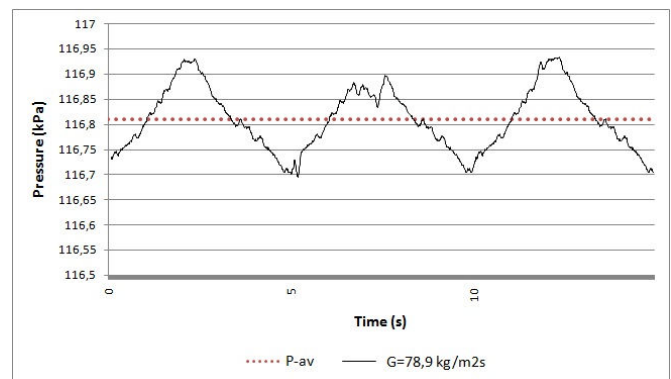


Figure 5: Pressure fluctuations in 0,254mm inner diameter microtube at $G=78,9 \text{ kg/m}^2\text{s}$ mass flux, $q''= 24,93 \text{ W/cm}^2$ heat flux. (Fluctuation period is approx. 5s)

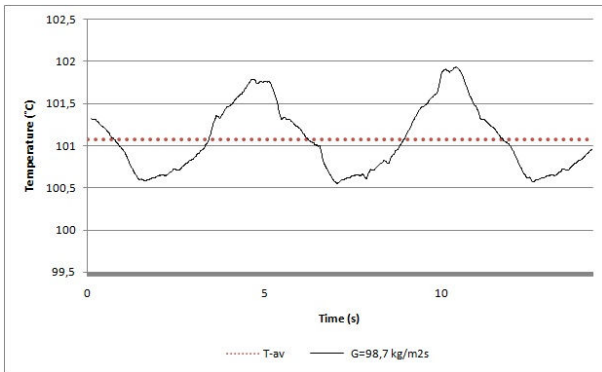


Figure 6: Temperature fluctuations in 0,254mm inner diameter microtube at $G=98,7 \text{ kg/m}^2\text{s}$ mass flux, $q''= 27,6 \text{ W/cm}^2$ heat flux, at Thermocouple 3. (Fluctuation period is approx. 5s)

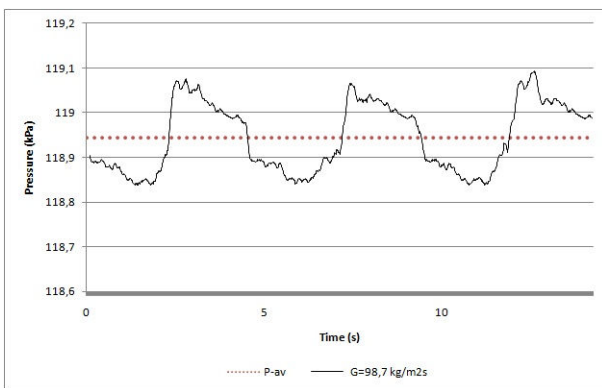


Figure 7: Pressure fluctuations in 0,254mm inner diameter microtube at $G=98,7 \text{ kg/m}^2\text{s}$ mass flux, $q''= 27,6 \text{ W/cm}^2$ heat flux. (Fluctuation period is approx. 5s)

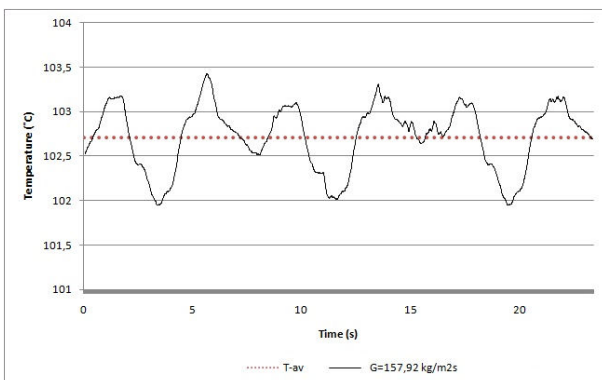


Figure 8: Temperature fluctuations in 0,254mm inner diameter microtube at $G=157,92 \text{ kg/m}^2\text{s}$ mass flux, $q''= 48 \text{ W/cm}^2$ heat flux, at Thermocouple 3. (Fluctuation period is approx. 8s)

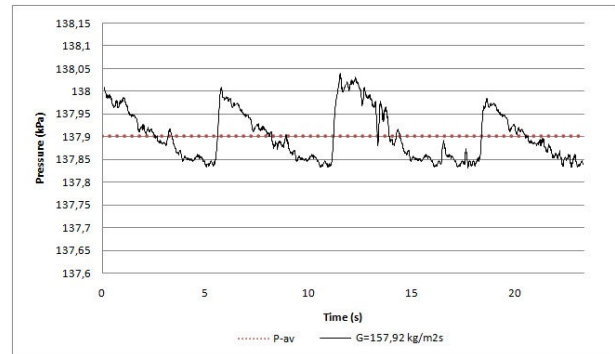


Figure 9: Pressure fluctuations in 0,254mm inner diameter microtube at $G=157,92 \text{ kg/m}^2\text{s}$ mass flux, $q''= 48 \text{ W/cm}^2$ heat flux. (Fluctuation period is approx. 6s)

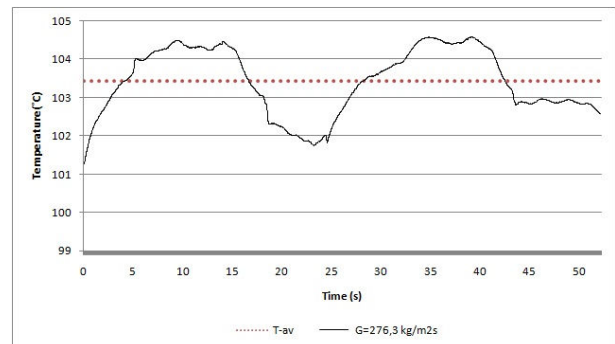


Figure 10: Temperature fluctuations in 0,254mm inner diameter microtube at $G=276,3 \text{ kg/m}^2\text{s}$ mass flux, $q''= 75,4 \text{ W/cm}^2$ heat flux, at Thermocouple 3. (Fluctuation period is approx. 25s)

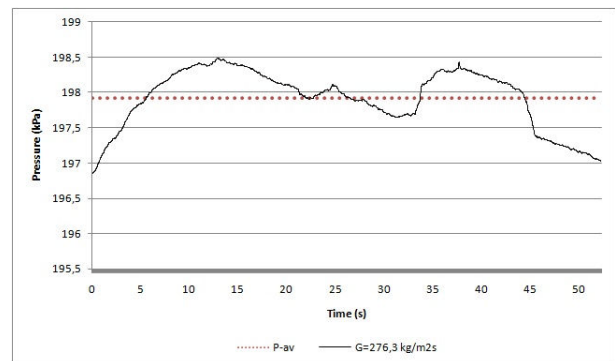


Figure 11: Pressure fluctuations in 0,254mm inner diameter microtube at $G=276,3 \text{ kg/m}^2\text{s}$ mass flux, $q''= 75,4 \text{ W/cm}^2$ heat flux. (Fluctuation period is approx. 25s)

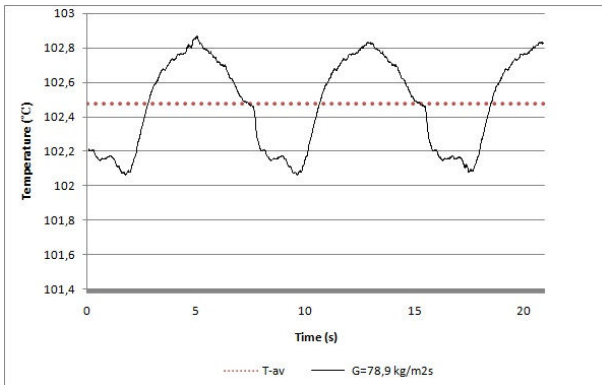


Figure 12: Temperature fluctuations in 0,254mm inner diameter valve-restricted microtube at $G=78,9 \text{ kg/m}^2\text{s}$ mass flux, $q''= 28,9 \text{ W/cm}^2$ heat flux, at Thermocouple 3. (Fluctuation period is approx. 7s)

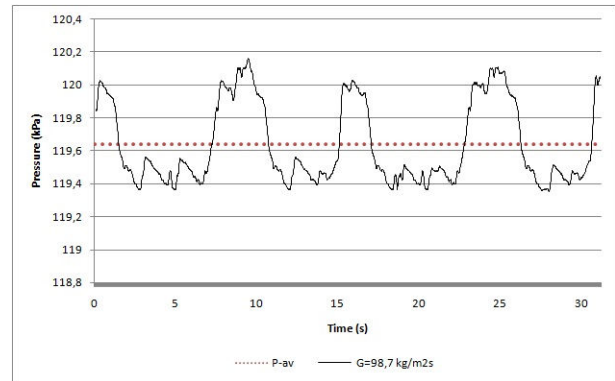


Figure 15: Pressure fluctuations in 0,254mm inner diameter valve-restricted microtube at $G=98,7 \text{ kg/m}^2\text{s}$ mass flux, $q''= 31,5 \text{ W/cm}^2$ heat flux. (Fluctuation period is approx. 14s)

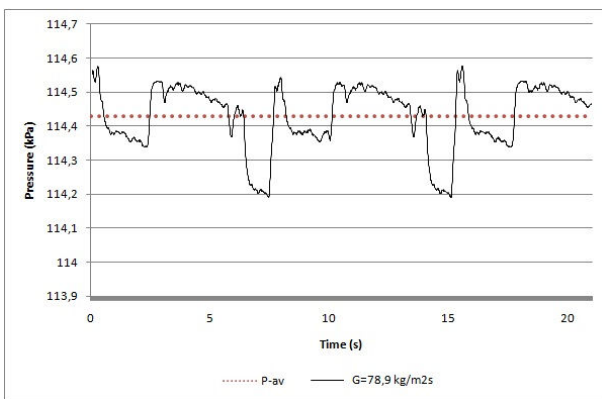


Figure 13: Pressure fluctuations in 0,254mm inner diameter valve-restricted microtube at $G=78,9 \text{ kg/m}^2\text{s}$ mass flux, $q''= 28,9 \text{ W/cm}^2$ heat flux. (Fluctuation period is approx. 7s)

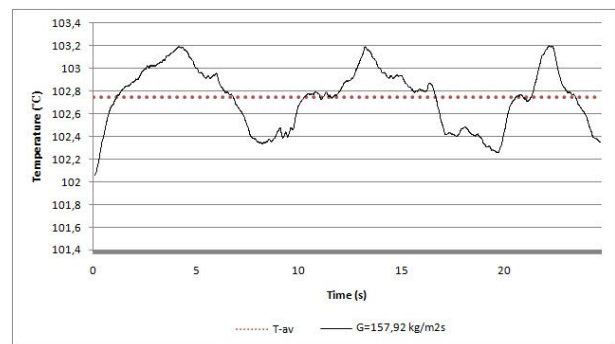


Figure 16: Temperature fluctuations in 0,254mm inner diameter valve-restricted microtube at $G=157,92 \text{ kg/m}^2\text{s}$ mass flux, $q''= 52 \text{ W/cm}^2$ heat flux, at Thermocouple 3. (Fluctuation period is approx. 15s)

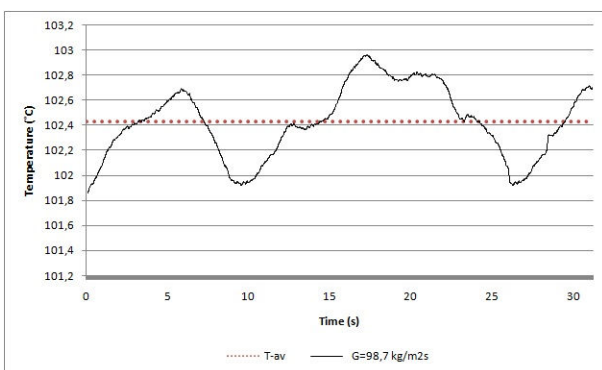


Figure 14: Temperature fluctuations in 0,254mm inner diameter valve-restricted microtube at $G=98,7 \text{ kg/m}^2\text{s}$ mass flux, $q''= 31,5 \text{ W/cm}^2$ heat flux, at Thermocouple 3. (Fluctuation period is approx. 13s)

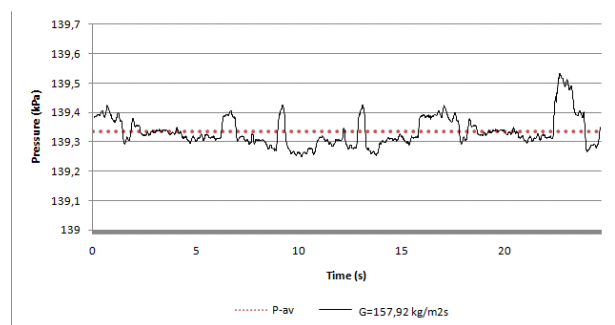


Figure 17: Pressure fluctuations in 0,254mm inner diameter valve-restricted microtube at $G=157,92 \text{ kg/m}^2\text{s}$ mass flux, $q''= 52 \text{ W/cm}^2$ heat flux. (Fluctuation period is approx. 7s)

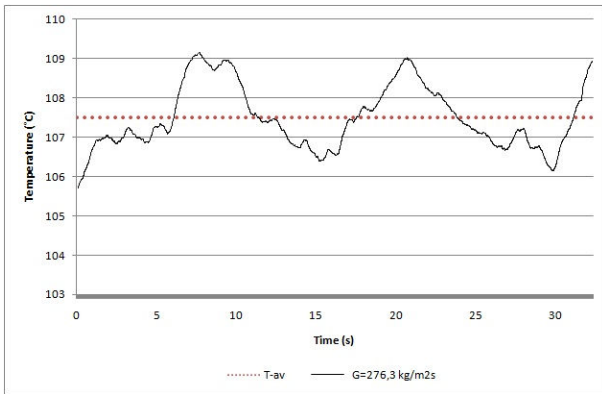


Figure 18: Temperature fluctuations in 0,254mm inner diameter valve-restricted microtube at $G=276,3$ $\text{kg/m}^2\text{s}$ mass flux, $q''=80,3$ W/cm^2 heat flux, at Thermocouple 3. (Fluctuation period is approx. 13s)

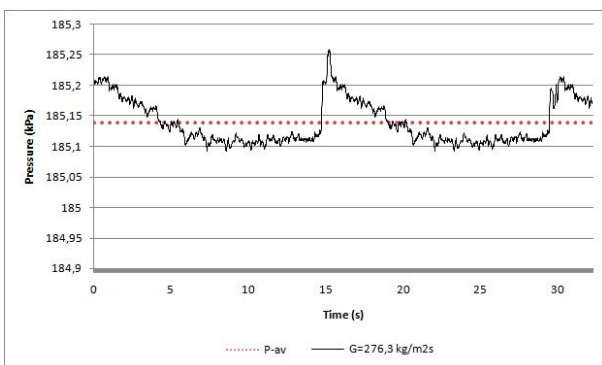


Figure 19: Pressure fluctuations in 0,254mm inner diameter valve-restricted microtube at $G=276,3$ $\text{kg/m}^2\text{s}$ mass flux, $q''=80,3$ W/cm^2 heat flux. (Fluctuation period is approx. 15s)

References

- [1] Barber, J., Sefiane, K., Brutin, D., Tadrist, L., 2009, "Hydrodynamics and Heat Transfer During Flow Boiling Instabilities in a Single Microchannel", *Applied Thermal Engineering*, 29, pp 1299-1308.
- [2] Kuo, C.J., Kosar, A., Peles, Y., Virost, S., Mishra, C., Jensen, M.K., 2006, "Bubble Dynamics During Boiling in Enhanced Surface Microchannels", *Journal of Microelectromechanical Systems*, 15(6), pp. 1514-1526.
- [3] Nuñez, M., Polley, G.T., Reyes, E., and Muñoz A., 1999, "Surface Selection and Design of Plate-Fin Heat Exchangers", *Applied Thermal Engineering*, 19, pp. 917-931.
- [4] Barber, J., Sefiane, K., Brutin, D., Tadrist, L., 2010, "Hydrodynamics, heat transfer and flow boiling instabilities in microchannels", University of Edinburgh – Engineering and Electronics PhD Thesis Collection.
- [5] Chang, M.H., Chen, F., and Fan, N-S., 2006, "Analysis of membraneless fuel cell using laminar flow in a Y-shaped microchannel, *Journal of power sources*, 159 (2), pp. 810-816.
- [6] Tabeling, P., "Introduction to Microfluidics", Oxford University Press, Ch.1, 2005.
- [7] Moriñigo, J.A., and Quesada J.H., 2010, "Solid-gas surface effect on the performance of a MEMS-class nozzle for micropropulsion", *Sensors and Actuators A: Physical*, 162(1), pp. 61-71.
- [8] Kosar, A., Ozdemir, M.R., and Keskinöz, M., 2010, "Pressure drop across micro-pin heat sinks under unstable boiling conditions", *International Journal of Thermal Sciences*, 49, pp. 1253-1263.
- [9] Wang, G., and Cheng, P., 2008, "An experimental study of flow boiling instability in a single microchannel", *International Communications in Heat and Mass Transfer*, 35(10), pp. 1229-1234.
- [10] Bogojevic, D., Sefiane, K., Walton, A.J., Lin, H., and Cummins, G., 2009, "Two-phase flow instabilities in a silicon microchannels heat sink", *International Journal of Heat and Fluid Flow*, 30(5), pp. 854-867.
- [11] Fukano, T., and Kariyasaki, L., 1993, "Characteristic of gas-liquid two-phase flow in a capillary tube", *Nucl. Eng. Des.*, 141, pp. 58-68.
- [12] Triplett, K. A., Ghiaasiaan, S.M., Abdel-Khalik, S.I., and Sadowski, D.L., 1999, "Gas-liquid two-phase flow in microchannels Part I: Two-phase flow patterns", *Int. J. Multiphase Flow*, 25(3), pp. 377-394.

- [13] Peng, X.F., Hu, H.Y., and Wang, B.X., 1998, "Boiling nucleation during liquid flow in microchannels", *Int. J. Heat Mass Transfer*, 41 (1), pp. 101–106.
- [14] Thome, J.R., Dupont, V., and Jacobi, A.M., 2004, "Heat transfer model for evaporation in microchannels. Part I : Presentation of the model", *Int. J. Heat Mass Transfer* 47, pp. 3375–3385.
- [15] Yan, Y., Kenning, D.R.B., 1998, "Pressure fluctuations during boiling in a narrow channel", HTFS Research Symposium.
- [16] Kenning, D.R.B., and Yan, Y., 2001, "Saturated flow boiling of water in a narrow channel, experimental investigation of local phenomena", *ICHEM Trans. A, Chem. Eng. Des.*, 79, pp. 425–436.
- [17] Brutin, D., Topin, F., and Tadrist, L., 2003, "Experimental study of the unsteady convective boiling in heated minichannels", *Int. J. Heat Mass Transfer*, 46, pp. 2957–2965.
- [18] Kennedy, J.E., Dowling, G.M. Roach Jr., Abdel-Khalik, M.F., Ghiaassiaan, S.I., Jeter, S.M., and Quershi, S.M., 2000, "The onset of flow instability in uniformly heated horizontal micro-channels", *J. Heat Transfer*, 122, pp. 118–125.
- [19] Kandlikar, S.G., Steinke, M.E., Tian, M.E., Campbell, L.A., 2001, "High-speed photographic observation of flow boiling of water in parallel mini-channels, In: Proc. 2001, National Heat Transfer Conference, Anaheim, CA", 10–12 June.
- [20] Kandlikar, S.G., 2002, "Fundamental issues related to flow boiling in minichannels and microchannels", *Exp. Therm. Fluid Sci.* 26 (2–4), pp. 389–407.
- [21] Hetsroni, G., Klein, D., Mosyyak, A., Segal Z., and Pogrebnyak, E., 2003, "Convective boiling in parallel micro-channels". In: Kandlikar, Editor, *First Int. Conf. Microchannels and Minichannels*, April 24–25, Rochester, ASME, New-York, USA, pp. 59–67.
- [22] Qu, W., and Mudawar, I., 2003, "Measurement and prediction of pressure drop in two-phase micro-channels heat sinks", *Int. J. Heat Mass Transfer* 46, pp. 2737–2753.
- [23] Consolini, L., Thome, J.R., 2009, "Microchannel convective heat transfer with flow instabilities", ECI International Conference on Boiling Heat Transfer Florianópolis-SC-Brazil, 3-7 May.
- [24] Kosar, A., Kuo, C.-J., Peles, Y., 2009, "Suppression of Boiling Flow Oscillations in Parallel Microchannels by Inlet Restrictors", *Journal of Heat Transfer*, 128(3), pp. 251-261.
- [25] Kuo, C.-J., Peles., 2008, "Flow Boiling Instabilities in Microchannels and Means for Mitigation by Reentrant Cavities", *Journal of Heat Transfer*, 130, pp. 072402-1
- [26] Barber, J., Sefiane, K., Brutin, D., Tadrist, L., 2010, "Bubble confinement in flow boiling of FC-72 in a "rectangular" microchannel of high aspect ratio", *Experimental Thermal and Fluid Science*, 34, pp. 1375-1388.
- [27] Bergles, A.E., Kandlikar, S.G., 2005, "On the Nature of Critical Heat Flux in Microchannels", *Journal of Heat Transfer*, 127, pp. 101.